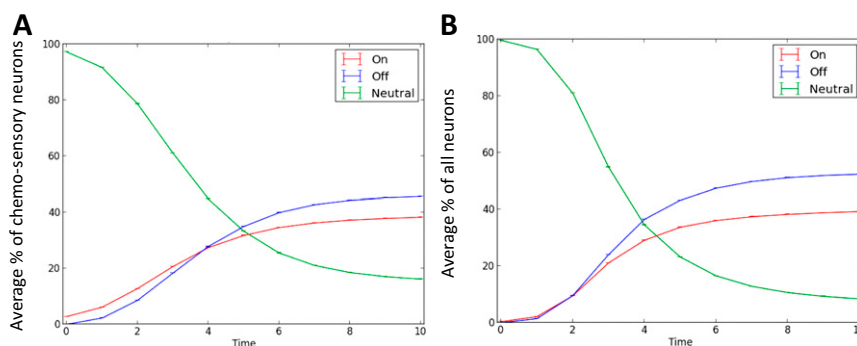
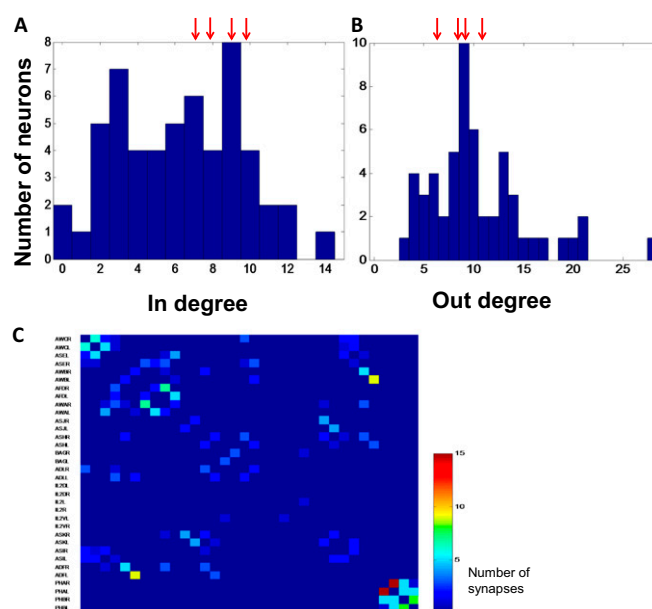


# Supporting Information

Zaslaver et al. 10.1073/pnas.1423656112



**Fig. S1.** Simulation results of signal propagation in the neural network showing that most of the neural network is expected to respond following activation of any single chemosensory neuron. We generated 10,000 networks preserving the known neural connectivity, but in each network a synapse is randomly assigned to be excitatory or inhibitory (with probability 0.5). At time point zero, one of the chemosensory neurons is activated, and the signal is then propagated in the network according to its assigned synapse types. The network starts with all neurons neutral (green, not activated nor inhibited), and as time progresses, we count the fraction of neurons that are activated (red) or inhibited (blue). After 10 discrete time steps of signal propagation, the network reaches a steady state. The curves are the average of simulations following activation of each of the chemosensory neurons across all 10,000 randomly generated. (A) Average fraction of chemo-sensory neurons only. (B) Average fraction of all neurons in the network.



**Fig. S2.** Chemosensory neurons that make up the top of the functional hierarchy are not hubs in the sensory system. Red arrows indicate the in-degree (A) and out-degree (B) of the top four neurons in the functional map:  $\{AWC^{ON}, AWC^{OFF}, ASEL, ASER\}$ . In-degrees,  $\{9, 7, 8, 10\}$ ; out-degrees,  $\{7, 9, 9, 11\}$ . Network wiring data are based on ref. 1. (C) Connectivity matrix based on number of synapses between pairs of chemosensory neurons. The order of the chemosensory neurons in the matrix matches the order that these neurons appear in the clustered functional map in Fig. 2. This connectivity matrix shows that connectivity alone cannot explain the hierarchical function of the chemosensory system. A connectivity bias is observed along the diagonal, emphasizing the tendency of symmetrical left and right pair of neurons to be anatomically wired.

1. Varshney LR, Chen BL, Paniagua E, Hall DH, Chklovskii DB (2011) Structural properties of the *Caenorhabditis elegans* neuronal network. *PLOS Comput Biol* 7(2):e1001066.

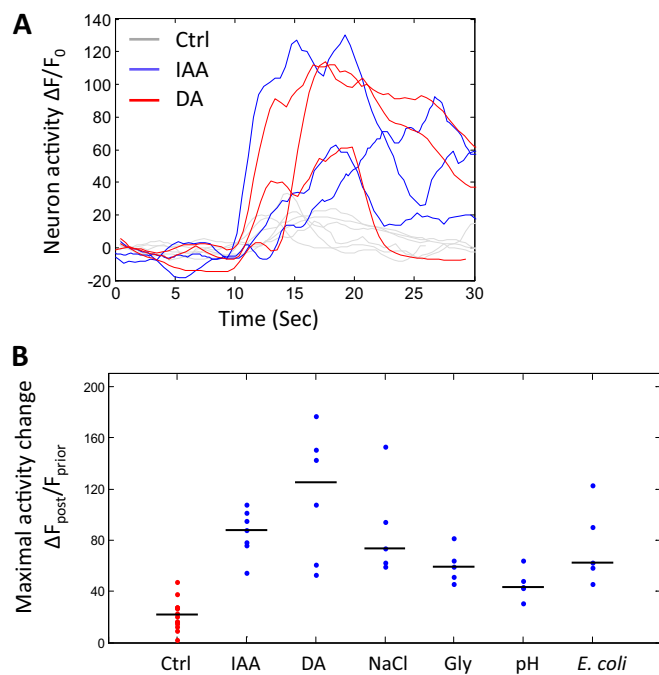


**Fig. 53.** Activity trace examples for the  $\text{AWC}^{\text{ON}}$  neuron. (A) Stimuli were switched ON/OFF at  $t = 10$  s: IAA (blue) and diacetyl (DA, red). In control experiments, where the same M9 buffer was used for both ON and OFF streams,  $\text{AWC}^{\text{ON}}$  mildly responds to the change of flow (Ctrl, gray). (B) Quantification of maximal responses for the  $\text{AWC}^{\text{ON}}$  neuron in the different conditions. Maximal response is calculated by subtracting the average intensity during the 5 s before the switch (time window of 5–10 s,  $F_{\text{prior}}$ ) from the maximal peak and then dividing by  $F_{\text{prior}}$  (multiplied by 100 for percentage). The maximal peak is the average intensity in the time window during 2 s before the point of maximal intensity to 2 s after that time point. The magnitude of the response to each of the stimuli is significantly higher than the response to the flow change alone. Ctrl,  $n = 14$ ; IAA,  $n = 7$ ,  $P < 10^{-8}$ ; DA,  $n = 6$ ,  $P < 10^{-5}$ ; NaCl,  $n = 5$ ,  $P < 10^{-4}$ ; Gly-1M,  $n = 5$ ,  $P < 10^{-4}$ ; pH,  $n = 5$ ,  $P < 0.005$ ; *E. coli*,  $n = 5$ ,  $P < 10^{-5}$ . The number of repeats is denoted by  $n$ , and  $p$  is the  $P$  value for each condition compared with the control. Vertical line is the median.

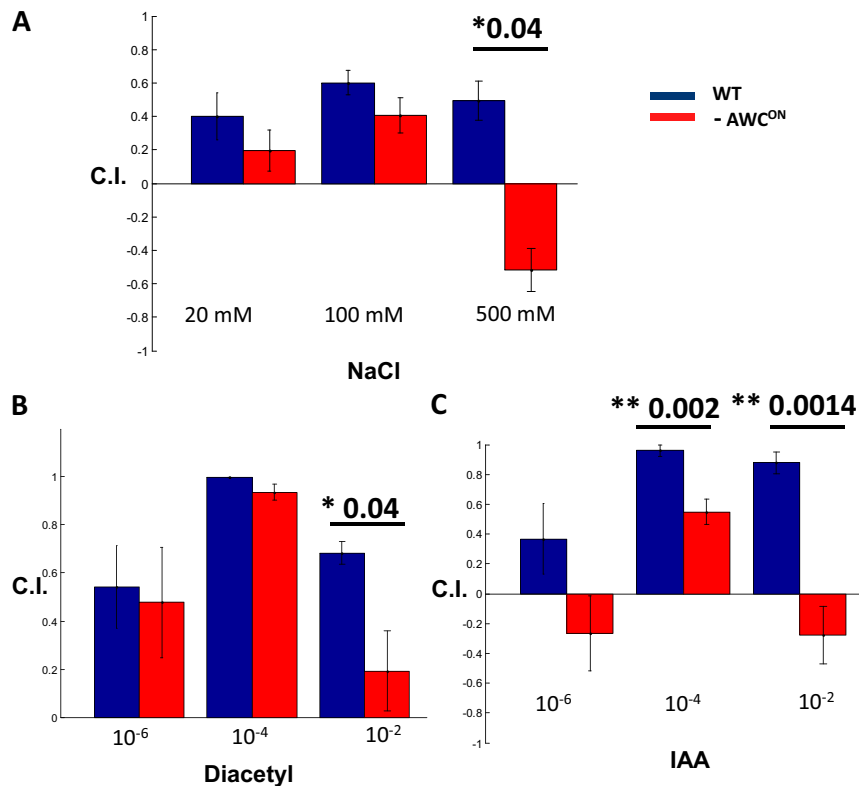


**Fig. S4.** Chemotaxis assays of N2 WT worms compared with AWC<sup>ON</sup> genetically ablated worms (PY7502) (1) toward different concentrations of (A) NaCl, (B) diacetyl, and (C) IAA. In all experiments, the Chemotaxis Index (C.I.) is an average of at least eight repeats with 10 worms per each repeat. Error bars are SEM.

1. Beverly M, Anbil S, Sengupta P (2011) Degeneracy and neuromodulation among thermosensory neurons contribute to robust thermosensory behaviors in *Caenorhabditis elegans*. *J Neurosci* 31(32):11718–11727.

**Table S1. List of the strains expressing GCaMP3 in target neurons used in this study**

Tagged neurons	Genotype	Strain name
AWC <sup>ON</sup>	<i>syEx1240[<i>str-2::GCaMP3+pha-1</i>]; pha-1(e2123ts); him-5(e1490)</i>	PS6374
AWC <sup>OFF</sup>	<i>syEx1238[<i>srsx-3::GCaMP3+pha-1</i>]; pha-1(e2123ts)</i>	PS6253
AWA	<i>syEx1252[<i>gpa-6::GCaMP3+pha-1</i>]; pha-1(e2123ts); him-5(e1490)</i>	PS6390
AWB	<i>syEx1245[<i>str-1::GCaMP3+pha-1</i>]; pha-1(e2123ts)</i>	PS6384
ASER	<i>syEx1243[<i>gcy-5::GCaMP3+pha-1</i>]; pha-1(e2123ts)</i>	PS6382
ASEL	<i>syEx1244[<i>gcy-7::GCaMP3+pha-1</i>]; pha-1(e2123ts)</i>	PS6383
AFD	<i>syEx1251[<i>gcy-8::GCaMP3+pha-1</i>]; pha-1(e2123ts)</i>	PS6389
ASH	<i>syEx1246[<i>sra-6::GCaMP3+pha-1</i>]; pha-1(e2123ts)</i>	PS6386
ASK	<i>syEx1247[<i>sra-9::GCaMP3+pha-1</i>]; pha-1(e2123ts); him-5(e1490)</i>	PS6387
ASI	<i>syEx1200[<i>gpa-4::GCaMP3+pha-1</i>]; pha-1(e2123ts)</i>	PS6410
ASJ	<i>syEx1248[<i>gpa-9::GCaMP3+pha-1</i>]; pha-1(e2123ts); him-5(e1490)</i>	PS6388
BAG	<i>syEx1206[<i>gcy-33::GCaMP3+pha-1</i>]; pha-1(e2123ts)</i>	PS6416
ADL	<i>sri-51::GCaMP3+pha-1; pha-1(e2123ts)</i>	PS6522
ADF	<i>syEx1249[<i>srh-142::GCaMP3+pha-1</i>]; pha-1(e2123ts)</i>	PS6377
PHA, PHB	<i>syEx1242[<i>osm-3::GCaMP3+pha-1</i>]; pha-1(e2123ts)</i>	PS6376
IL-2, FLP, PVD, PVC	<i>syEx1237[<i>des-2::GCaMP3+pha-1</i>]; pha-1(e2123ts)</i>	PS6252
ADE, PDE, CEP	<i>syEx1236[<i>dat-1::GCaMP3+pha-1</i>]; pha-1(e2123ts)</i>	PS6250
OLQ	<i>syEx1250[<i>ocr-4::GCaMP3+pha-1</i>]; pha-1(e2123ts)</i>	PS6378
AVM, ALM, PVM, PLM	<i>syEx1254[<i>mec-4::GCaMP3+pha-1</i>]; pha-1(e2123ts)</i>	PS6393